BOARD # 476: Modern Tools for Engineering Education Based on Virtual Laboratories

Dr. Danielle Sami Nasrallah PhD. eng., OPAL-RT Technologies

Danielle Sami Nasrallah received her Bachelor's degree in electromechanical engineering and the Diplôme d'Études Approfondies in electrical engineering from the École supérieure d'ingénieurs de Beyrouth (´ESIB), Beirut, Lebanon, in 2000 and 2002, respectively, and Ph. D. degree in Robotics from McGill University, Montreal, QC, Canada, in 2007. During her Ph.D. studies, she worked on a part-time basis at Robotics Design as a control and robotics engineer. She moved to Meta Vision Systems in 2006- 2007 as a control and applications engineer. In 2008 she joined the electrical department of the Royal Military College of Kingston as an assistant professor, and, in 2009, she was a visiting assistant professor at the American University of Beirut. From 2010 to 2014, she worked as a consultant in control and systems engineering. In 2014 she joined OPAL-RT Technologies where she is currently Courseware Lead & SME Robotics. She also had links with academia as she is a lecturer at Concordia University in Canada, JUNIA in France, and ESIB in Lebanon. Additionally, she intervenes in lectures at H-BRS Germany.

Mr. Angelo Antoine Chrabieh, OPAL-RT Technologies

Angelo Chrabieh received his bachelor's degree in electrical engineering from the École supérieure d'ingénieurs de Beyrouth (ESIB), Saint-Joseph University of Beirut, Lebanon, in 2023.

He joined OPAL-RT as an intern in Summer 2022, then he did his FYP with OPAL-RT in Winter 2023.

Since August 2023 Angelo has been working as a junior Courseware Analyst at OPAL-RT Technologies, where he contributes to the development and maintenance of electric and robotics real-time virtual laboratories

Dr. Wolf Peter Jean Philippe, OPAL-RT Technologies

Wolf Peter Jean Philippe received his Bachelor's degree in electromechanical engineering from the Faculté des Sciences, Université d'État d'Haïti (FDS-UEH), Haiti, in 2012, and his M.Sc. degree in electrical engineering and his Ph.D. degree in electrical and computer engineering from Syracuse University, Syracuse, NY, USA, in 2015 and 2020, respectively. His primary research interests encompass demand response, modeling wind power generation, and the operation and control of power systems with a high penetration of wind energy resources. He is a Senior Courseware Analyst at OPAL-RT Technologies, where he leads the development of electric real-time virtual laboratories focused on power electronics, motor drives, renewable energy resources, and microgrid control and operation, among other topics.

Mr. Georges Henri Haddad, Opal-RT Technologies

Georges Henri Haddad received his Bachelor's degree in mechanical engineering from the École supérieure d'ingénieurs de Beyrouth (ESIB), Saint-Joseph University of Beirut, Lebanon in 2023. He joined OPAL-RT as an intern in Summer 2022, then he did his FYP with OPAL-RT in Winter 2023. Since August 2023 Georges has been working as a junior Courseware Analyst at OPAL-RT Technologies, where he contributes to the development and maintenance of robotics real-time virtual laboratories, featuring (i) serial robotics manipulators, (ii) parallel robotics manipulators, (iii) wheeled mobile robots, and (iv) autonomous off-road vehicles.

Modern Tools for Engineering Education Based on Virtual Laboratories

Dr. Danielle Sami Nasrallah PhD. eng., OPAL-RT Technologies

Danielle Sami Nasrallah received her Bachelor's degree in electromechanical engineering and the Diplôme d'Études Approfondies in electrical engineering from the École supérieure d'ingénieurs de Beyrouth (´ESIB), Beirut, Lebanon, in 2000 and 2002, respectively, and Ph. D. degree in Robotics from McGill University, Montreal, QC, Canada, in 2007. During her Ph.D. studies, she worked on a part-time basis at Robotics Design as a control and robotics engineer. She moved to Meta Vision Systems in 2006- 2007 as a control and applications engineer. In 2008 she joined the electrical department of the Royal Military College of Kingston as an assistant professor, and, in 2009, she was a visiting assistant professor at the American University of Beirut. From 2010 to 2014, she worked as a consultant in control and systems engineering. In 2014 she joined OPAL-RT Technologies where she is currently Courseware Lead & SME Robotics. She also had links with academia as she is a lecturer at Concordia University in Canada, JUNIA in France, and ESIB in Lebanon. Additionally, she intervenes in lectures at H-BRS Germany.

Mr. Angelo Antoine Chrabieh, OPAL-RT Technologies

Angelo Chrabieh received his bachelor's degree in electrical engineering from the École supérieure d'ingénieurs de Beyrouth (ESIB), Saint-Joseph University of Beirut, Lebanon, in 2023.

He joined OPAL-RT as an intern in Summer 2022, then he did his FYP with OPAL-RT in Winter 2023.

Since August 2023 Angelo has been working as a junior Courseware Analyst at OPAL-RT Technologies, where he contributes to the development and maintenance of electric and robotics real-time virtual laboratories

Dr. Wolf Peter Jean Philippe, OPAL-RT Technologies

Wolf Peter Jean Philippe received his Bachelor's degree in electromechanical engineering from the Faculté des Sciences, Université d'État d'Haïti (FDS-UEH), Haiti, in 2012, and his M.Sc. degree in electrical engineering and his Ph.D. degree in electrical and computer engineering from Syracuse University, Syracuse, NY, USA, in 2015 and 2020, respectively. His primary research interests encompass demand response, modeling wind power generation, and the operation and control of power systems with a high penetration of wind energy resources. He is a Senior Courseware Analyst at OPAL-RT Technologies, where he leads the development of electric real-time virtual laboratories focused on power electronics, motor drives, renewable energy resources, and microgrid control and operation, among other topics.

Mr. Georges Henri Haddad, Opal-RT Technologies

Georges Henri Haddad received his Bachelor's degree in mechanical engineering from the École supérieure d'ingénieurs de Beyrouth (ESIB), Saint-Joseph University of Beirut, Lebanon in 2023. He joined OPAL-RT as an intern in Summer 2022, then he did his FYP with OPAL-RT in Winter 2023. Since August 2023 Georges has been working as a junior Courseware Analyst at OPAL-RT Technologies, where he contributes to the development and maintenance of robotics real-time virtual laboratories, featuring (i) serial robotics manipulators, (ii) parallel robotics manipulators, (iii) wheeled mobile robots, and (iv) autonomous off-road vehicles.

Modern Tools for Engineering Education Based on Virtual Laboratories

1 Introduction

Education has always been a cornerstone of civilization. Modernization in educational tools is a must to maintain this cornerstone. This is also applicable to engineering education. Therefore, modern engineering education must move beyond traditional knowledge acquisition to emphasize practical applications and real-world experience. Virtual learning tools, specifically virtual laboratories, play a crucial role in this shift by offering hands-on learning opportunities through realistic simulations. These virtual laboratories enable students to test, experiment, and refine their skills in environments that closely mimic real-world conditions.
This paper will focus on four virtual laboratories, where two cover electrical applications and the other two cover robotics one. It should be noted that the focus here is on virtual laboratories, not remote ones, the distinction being well explained in [1]. The justification behind selecting these four labs out of the 35 that have been developed already goes like this:

- The concept of inverted classroom is known in education [2]. The synchronous machine virtual laboratory is doing exactly the same in terms of laboratory. So it can be perceived as an application to the inverted classroom concept. For that, a virtual electric machine test bench has been developed, replicating exactly its real counterpart, which is located at LEEPCI[1], Laval University[2]. This allows students to do the lab experiments in the comfort of their place before showing up in front of the real test bench. Therefore, they know the results in advance and they practiced the procedure already. Moreover, the testbench is equipped with fuses that will blow up in case a faulty maneuver occurred. For instance, if connection of the synchronous machine to the grid is activated while voltages from grid and stator are not almost in phase, fuses will blow up, obliging students to repeat the maneuver, thus mastering the procedure in advance. A survey on this new experience has been conducted at the end of the term and results are shown.

- The complexity of doing real experiments for educational purposes. The microgrid virtual laboratory exemplifies how such challenges can be addressed effectively. Indeed, as the world shifts toward cleaner and more sustainable energy solutions, the need for innovative educational tools in renewable energy has never been greater [3-5]. Virtual laboratories, enhanced by real-time simulations, are emerging as powerful resources for teaching and research in

[1]Laboratoire d'Électrotechnique, Électronique de Puissance et Commande Industrielle: http://leepci.gel.ulaval.ca/

[2]https://www.ulaval.ca/

this field. These advanced digital platforms provide students and researchers with a safe, controlled, and dynamic environment where they can experiment with microgrid operations, test control strategies, and analyze system performance without the limitations of physical laboratory setups. Numerous studies [6-10] highlight the benefits of virtual laboratories in renewable energy education. They enable learners to visualize complex power system behaviors, reinforce theoretical knowledge through practical application, and develop critical problem-solving skills. However, despite these advantages, many existing virtual labs suffer from high complexity and limited interactivity, making them challenging to use effectively. To address these challenges, this lab presents a scalable and user-friendly virtual laboratory specifically designed for real-time microgrid operations. Unlike traditional setups, this platform prioritizes accessibility and engagement, allowing students to interact with system components in real time, conduct experiments, and simulate real-world grid scenarios with greater ease, but without diluting content. By simplifying laboratory maneuvers that would typically be complex and time-consuming in a physical setting, this approach fosters a more intuitive and immersive learning experience. By integrating such virtual laboratories into renewable energy curricula, educators can better prepare students for the evolving energy industry. These tools not only bridge the gap between theory and practice but also empower future engineers to develop the skills and confidence needed to design, operate, and optimize sustainable power systems.

- The non-availability of experimental material. The robotics market is growing substantially but the academia didn't follow this pace. Therefore, many engineering institutions teach robotics without having a robotics laboratory. Additionally, there are not many institutions as that dedicating a Robotics department. Having said that, virtual robotics laboratories become a need to solve this unavailability matter. It worths noticing that the idea of virtual serial robotics manipulators is not new at all. Robots manufacturers have their own software packages. We can cite for example RoboGuide from FANUC[3]. However, these packages work with their corresponding robots only. The UR10e virtual laboratory is designed to allow student to manipulate the virtual UR10e robot as if they have it physically in front of them. Therefore, direct and inverse displacement analysis can be achieved while interacting with the virtual robot. Moreover, the Jacobian analysis putting the emphasis on (i) robot's configuration that become singular and (ii) robot's workspace that won't be respected are explained and shown live, allowing thus students to go to these restricted areas without worrying about braking the robot. Furthermore, trajectory generation algorithms used in pick-and-place operation are instantly validated by checking the robot motion when successfully grasping an object and moving it from point A to point B. Other analysis related to dynamics, force-based control can also be achieved bringing the regular

[3]https://www.fanucamerica.com/products/robots/robot-simulation-software-FANUC-ROBOGUIDE

'Introduction to Robotics' course beyond its heavy mathematic framework.

- The rapid control prototyping for challenging systems with unstable zero dynamics. Mobile wheeled pendulum laboratory is a perfect example. Prototype of MWP has been developed previously [11]. However, special care was given to the design by adding protective torus because this system suffers from unstable zero dynamics and its stabilization is tricky. Therefore, it will fall down if the controller is not well adjusted and electronics on board might be affected after several drops. Having said that, if students are given the possibility to test their controllers on a virtual prototype instead of implementing it directly on the physical one, this will save many damages, sparing the real prototype to the controller that attained maturity level. The virtual laboratory of MWP offers this opportunity as the virtual prototype is the digital twin of the real one and results of virtual versus real prototype performances are shown.

For the virtual laboratory experience to be successful and fulfill one or more of the four needs listed above, it is imperative that it contains the following features.

1. Interactivity: Students interact in real-time with systems to apply control and setpoints and obtain live plots and results.
2. Real thing: labs should not be perceived as video games and students must carefully plan their experiments, otherwise virtual fuses will blow up and protection will be engaged.
3. Instant Reset & Repeatability: Mistakes can be reset, and tests can be repeated under identical conditions for consistency.
4. Flexibility: students can change the configuration of the testbench by connecting/disconnecting components to exhibit a given behavior
5. Self-learning: Students can acquire knowledge at their own pace. Unlike physical labs, which often follow predefined procedures, virtual environments let students modify parameters, try new configurations, and discover unexpected results.
6. Accessibility: Students can run the laboratories on their laptop without the need for sophisticated hardware.
7. Scaling Experiments: Simulations allow for testing large-scale systems that would be impractical to set up in real life.
8. Cost Efficiency, no need for expensive hardware, reducing the financial burden on institutions and students.
9. Safety: Students can experiment with high voltages, currents, or hazardous conditions without risk.
10. Bridging Theory and Practice, interactive exercises help students understand theoretical concepts before working with real hardware.

In terms of paper organization, Section 2 provides an overview of the virtual laboratory of synchronous machines, while Section 3 focuses on the virtual laboratory of the microgrid. Section 4 discusses the UR10e serial manipulator , and Section 5 examines the virtual laboratory of a wheeled mobile pendulum. Section 6 presents a comprehensive list of all virtual laboratories developed within this framework, and Section 7 offers conclusions along with suggestions for future research directions.

2 Synchronous Machine Virtual Laboratory

2.1 Description of the Synchronous Machine Test Bench

The virtual test bench of the synchronous machine is shown in Fig. 1. It includes a DC machine, the three-phase synchronous wound rotor machine under study, controllable DC and AC power sources, variable passive loads, fuses, switches, and measurement instruments.

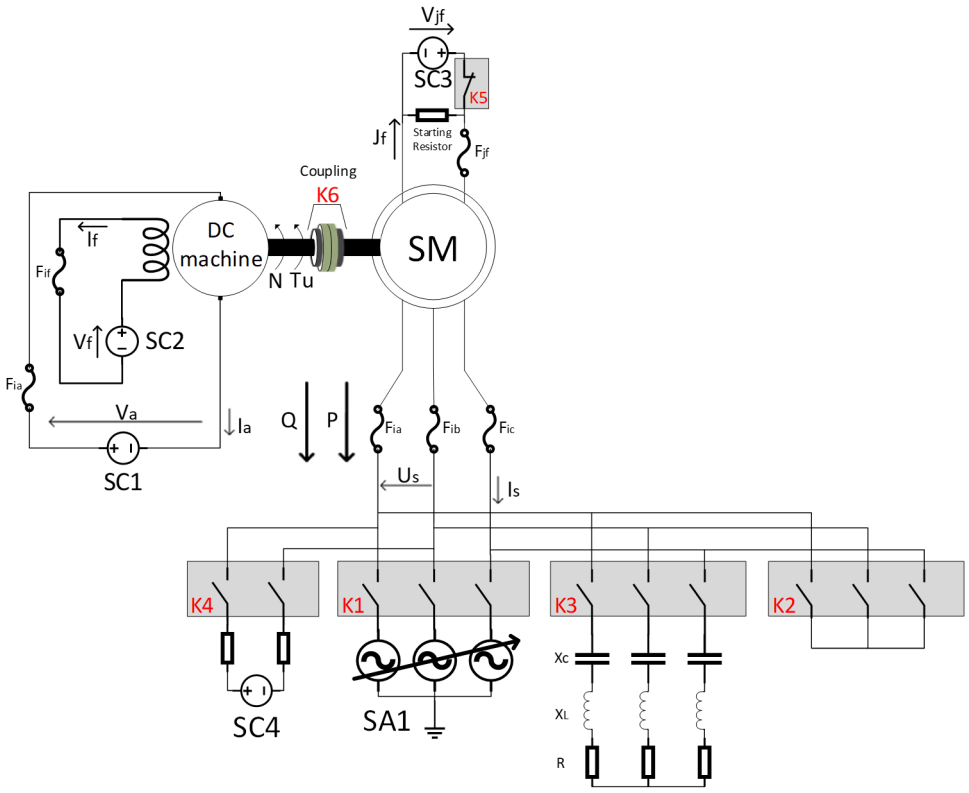

Figure 1: Virtual test bench of the synchronous machine

The corresponding machine nameplates are given in Tables 1 and 2

Parameter	Value	Description
S_n	10200 VA	Apparent nominal power
U_n	460 V	Nominal line-line effective voltage
J_{fn}	10.14 A	Field current to obtain Un no load at no-load and N_n
f_n	60 Hz	Nominal frequency
N_n	1800 RPM	Nominal speed

Table 1: Synchronous machine nameplate

Parameter	Value	Description
P_n	16 HP	Nominal power
V_{an}	460 V	Armature nominal voltage
V_{fn}	460 V	Field nominal voltage
I_{fn}	1.11 A	Field nominal current
N_n	1746 RPM	Nominal speed

Table 2: DC machine nameplate

2.2 Suggested Laboratory Exercises

Five laboratory exercises are suggested, namely:

- Identification of parameters of the steady-state synchronous machine model [12]
- Synchronous generator not connected to the grid feeding a passive load
- Synchronous generator connected to the grid
- Synchronous motor
- Standardized three-phase bolted fault and recovery voltage [13].

It is worth noticing that the testbench is designed in a versatile way, allowing users to go beyond these exercises. In the sequel, the synchronous generator connected to the grid exercise is elaborated, for which the corresponding GUI is shown in Fig. 2.

2.3 Exercise Example: Connecting the Generator to the Grid

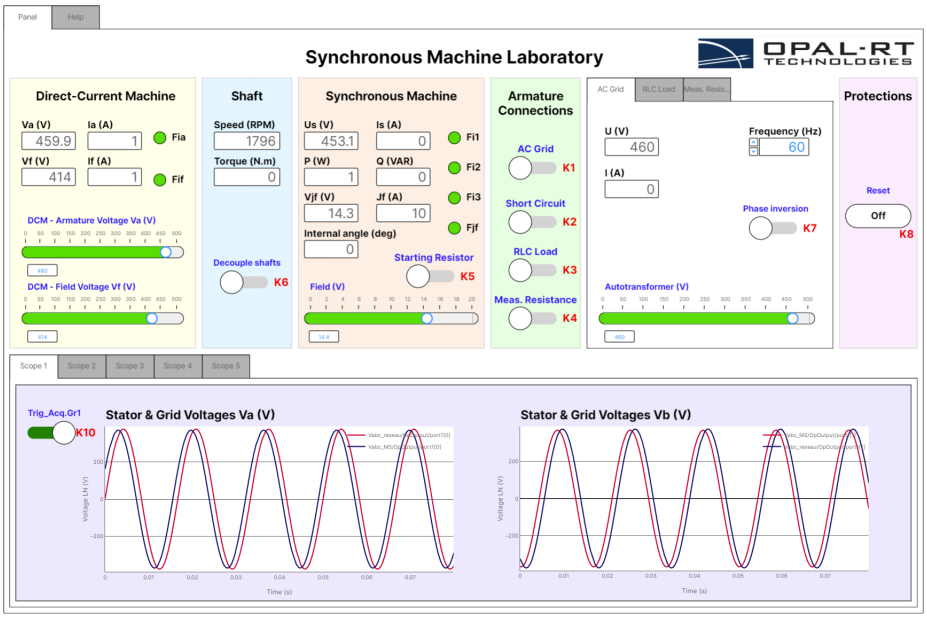

Figure 2: Connecting the generator to the grid

The maneuver to connect the synchronous machine to the grid is described here:

1. Gradually increase the field voltage of the DC machine from 0 to 414 V.
2. Gradually increase the armature voltage of the DC machine from 0 to 460 V.
3. Make sure that the speed is around 1790 RPM.
4. Increase gradually the field voltage of the synchronous machine from 0 to 14.4 V in such a way that the synchronous machine stator voltage U_s become close to 460 V while staying below it, i.e., around 455 V.
5. Gradually increase the grid voltage to 460 V using the autotransformer.
6. Select the tab corresponding to Scope 1 and activate the corresponding trigger by clicking on Switch K_{10}.
7. Observe the Stator and Grid voltages of Phases A and B in the scopes. Make sure they evolve in the same way (if not, use K_7 to achieve phase inversion). Close the switch K_1 when the instantaneous voltages are very close to each other, as shown above.
8. If the connection is achieved properly, the synchronous machine speed and stator voltages will be dictated by the grid as 1800 RPM and 460 V, respectively. If not, fuses will blow up and all values will decrease to zero. You have to restart the maneuver.

Once the connection is done, the user will increase/decrease the field voltage of

the DC machine, which will change the load at the coupling and consequently the power flow as summarized in the table.

V_f (V)	P (W)	Q (VAR)	Va (V)	Ia (A)	Speed (RPM)	Torque (N.m)	Angle (deg)
413	-2	-62	460	1	1800	0	0
410	997	-177	460	3.2	1800	5.3	5.8
405	2594	-705	460	6.9	1800	14.1	15.6
400	4101	-1709	460	10.6	1800	22.6	26.2
395	5492	-3474	460	14.3	1800	30.8	39.7
392	6185	-5769	460	16.5	1800	35.7	54.7
415	-685	-72	460	-0.5	1800	-3.6	-3.9
420	-2455	-439	460	-4.2	1800	-12.8	-14.5
423	-3568	-961	460	-6.4	1800	-18.4	-21.8
427	-5135	-2271	460	-9.4	1800	-26	-34.1
430	-6516	-5198	460	-11.6	1800	-31.7	-55

Table 3: Results of the regulation of the active power flow between the synchronous machine and the grid

By analyzing the values and signs of the above parameters, it can be concluded that a decrease in V_f results in an increase in active power, torque, and angle, whereas an increase in V_f has the opposite effect. Additionally, varying the V_f enables the identification of the ”floating point,” which occurs when the power flow between the two machines reaches zero. This can be observed when the torque becomes equal to zero. The test procedure and results are comparable to those obtained from experiments conducted in a physical laboratory.

2.4 Students Survey

A group of 22 students who used the virtual laboratory of synchronous machines was surveyed. The list of questions and answers is compiled below:

Questions	Yes	No
Did you appreciate this new tool in terms of understanding the subject matter?	100%	0%
Did you use this new tool to explore new experiments or to verify the theory?	45.5%	54.5%
Do you think that the concept can be extended to Fundamentals of Electrical Engineering course?	95.4%	4.6%

Table 4: Students Survey Results

In addition, students were asked to specify the percentage of time to allocate to

virtual laboratories versus real ones. The results are shown in the following diagram:

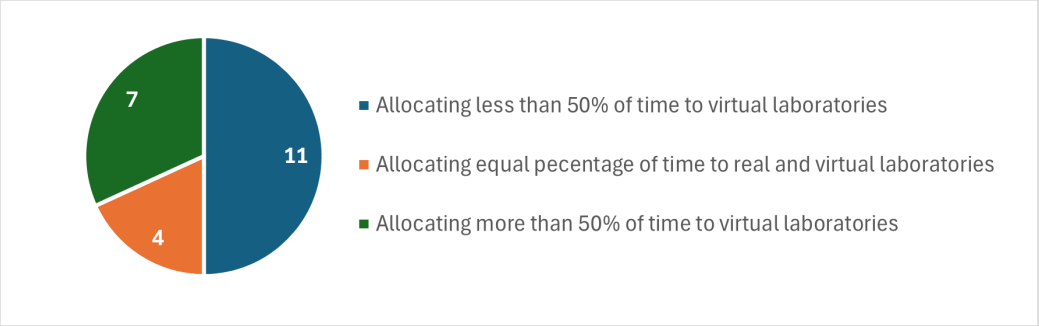

Figure 3: Student preferences for laboratory time distribution: virtual vs. real labs

3 Microgrid Virtual Laboratory

The microgrid test bench [14], illustrated in Fig. 4, integrates several key components: a wind turbine generation system (WTGS) [15], a photovoltaic generation system (PVGS) [16], and a 60 kW lithium-ion battery energy storage system (BESS) [17]. The WTGS is connected to the microgrid via a 50 kVA transformer, while the PVGS is connected through a three-phase inverter and a 14.4 kVA transformer. The BESS connects to the microgrid through a three-phase inverter and a 72 kVA transformer. The demand for the microgrid load is represented by three distinct loads: the first is a hospital, the second is a combination of critical load demands, and the third is a fully sheddable residential load. The microgrid controller ensures the stability of the system by balancing power generation with varying load demands.

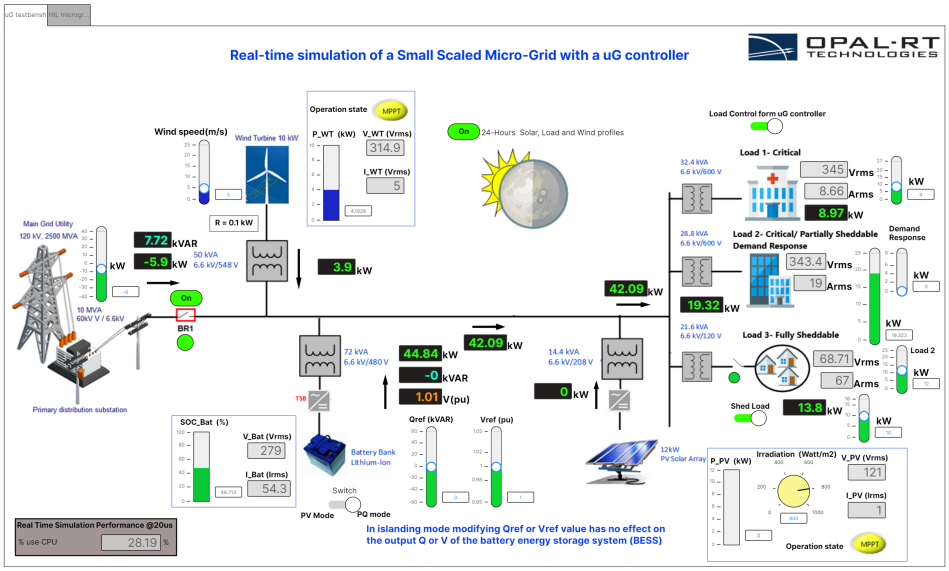

Figure 4: Schematic representation of the microgrid

The microgrid is capable of operating in two distinct modes:

- Mode 1: Connected to the main grid utility.
- Mode 2: Operating independently from the main grid utility, referred to as the islanded mode.

The laboratory setup supports testing in both operational modes and allows for the adjustment of various parameters within the simulation. These include solar intensity, wind speed, grid power, and load configurations, providing a versatile platform for comprehensive analysis and experimentation. In addition, the laboratory facilitates conducting a 24-hour test, simulating a full day-night cycle. During this test, the Sun rises and sets, and wind speeds vary, enabling observation of the system's behavior under dynamic conditions. Fig. 5 illustrates the 24-hour profiles for solar irradiance, load demand, and wind speed.

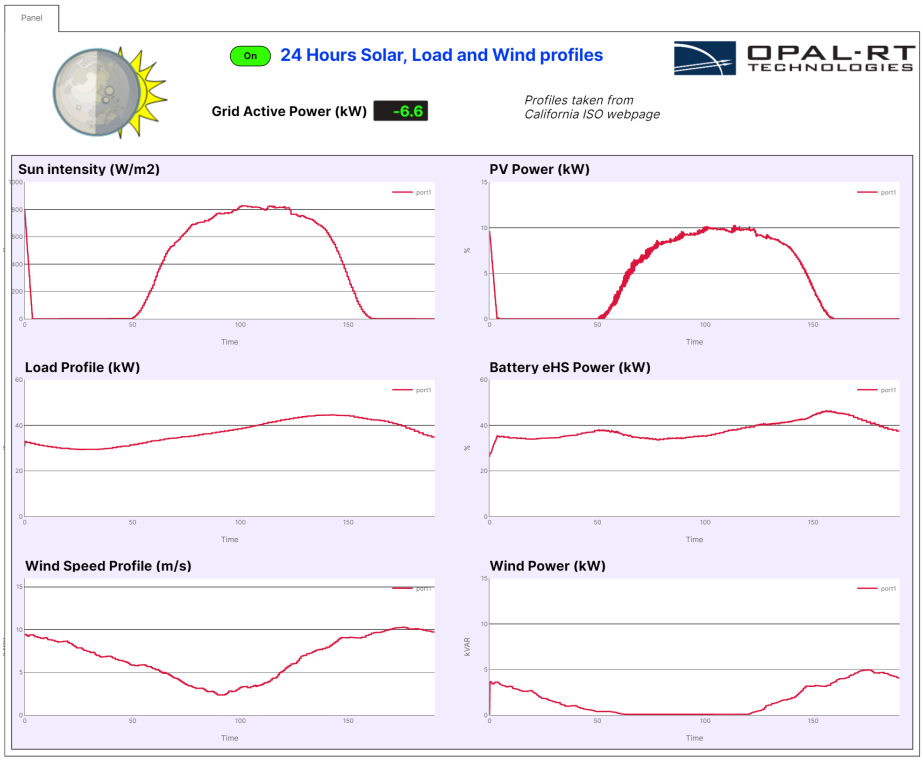

Figure 5: 24 Hours solar, load and wind profiles

A series of tests were performed in islanded mode to evaluate the system's behavior under varying operating conditions. These conditions were achieved by adjusting wind speed, solar irradiance, and load powers, with the corresponding source and load data recorded at each operating point. The results are shown in Table 5.

Wind Speed (m/s)	**Irradiance (W/m^2)**	**P_{wind} (KW)**	**P_{solar} (KW)**	**$P_{battery}$ (KW)**	**P_{load1} (KW)**	**P_{load2} (KW)**	**P_{load3} (KW)**	**Total**	
								P_{source}	**P_{load}**
5	800	0	9.62	21.23	8.97	11.94	9.94	30.85	30.85
5	600	0	7.08	23.77	8.97	11.94	9.94	30.85	30.85
5	300	0	3.35	27.50	8.97	11.94	9.94	30.85	30.85
10	300	4.32	3.35	23.18	8.97	11.94	9.94	30.85	30.85
12	300	6.90	3.35	20.60	8.97	11.94	9.94	30.85	30.85
15	300	10.03	3.35	17.47	8.97	11.94	9.94	30.85	30.85
12	600	10.03	7.08	20.52	15.75	11.94	9.94	37.63	37.63
12	600	10.03	7.08	22.59	15.75	14.01	9.94	39.70	39.70
12	600	10.03	7.08	25.09	15.75	11.94	14.51	42.20	42.20

Table 5: Simulation results for different wind speeds, irradiance levels and loads

The data clearly demonstrate that total power generation consistently matches total load demand, maintaining a balanced system.

4 UR10e Serial Manipulator Virtual Laboratory

The serial manipulator UR10e is a 6-dof spatial manipulator. Therefore, it is composed of six links and six revolute joints, namely, the base, shoulder, elbow, and three wrist joints. A frame is associated with each link, where $\mathcal{F}_1$ is linked to the fixed base link, etc., until $\mathcal{F}_7$ which is linked to the 6^{th} link, as shown in Fig. 6(a). The notation adopted for serial robotic manipulators is based on the one in [18]. Additionally, a gripper has been added for pick-and-place operations, as shown in Fig. 6(b).
The corresponding DH-Table for this robot is given in Table 6.

i	a_i [m]	b_i [m]	α_i [rad]	θ_i [rad]
1	0	0.1273	$\frac{\pi}{2}$	π
2	0.6127	0	0	$\frac{\pi}{2}$
3	0.5723	0	0	0
4	0	0.163941	$\frac{\pi}{2}$	π
5	0	0.1157	$\frac{\pi}{2}$	$-\frac{\pi}{2}$
6	0	0.0922	0	0

Table 6: UR10e DH table

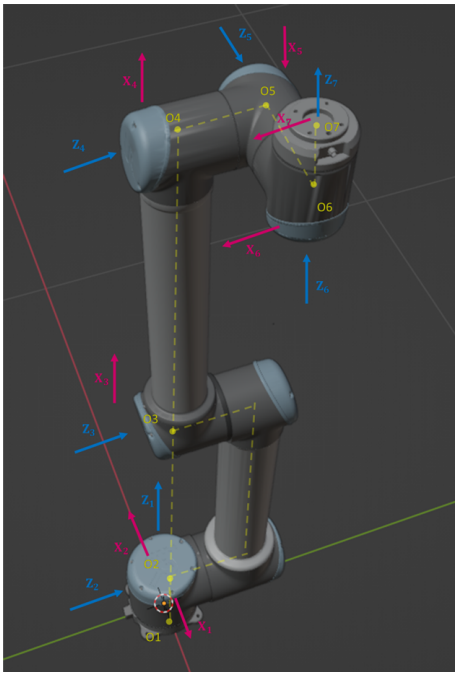

(a) UR10e serial manipulator with its associated frames

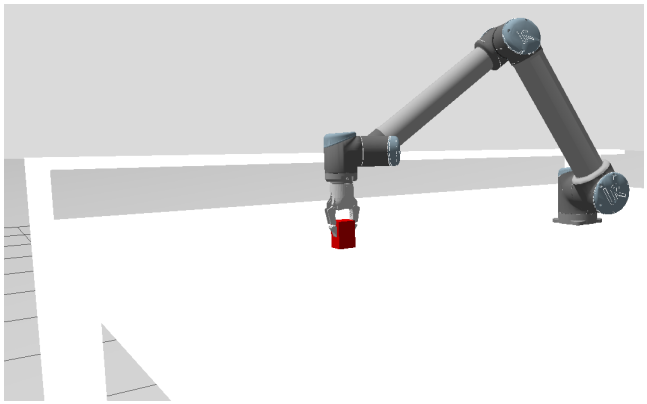

(b) UR10e operating on a table and grasping a cube

Figure 6: UR10e

For an architecture to be decoupled, which allows the decoupling of the orientation problem from the positioning one, the three following parameters must be zero, i.e., $a_4 = a_5 = b_5 = 0$. From the DH table shown above, it is clear that UR10e has a non-decoupled architecture, which renders the direct and inverse displacement analysis more challenging.

Moreover, the vector $\mathbf{a}_i$ represents the position vector that connects the origin O_i of $\mathcal{F}_i$ to the origin O_{i+1} of $\mathcal{F}_{i+1}$, while the rotation matrix $\mathbf{Q}_i$ represents the orientation

of $\mathcal{F}_{i+1}$ with respect to $\mathcal{F}_i$. The expressions of $\mathbf{a}_i$ and $\mathbf{Q}_i$ are as follows:

$$\mathbf{a}_i \equiv [\mathbf{a}_i]_i = \begin{bmatrix} a_i \cos\theta_i \\ a_i \sin\theta_i \\ b_i \end{bmatrix}, \ \mathbf{Q}_i \equiv [\mathbf{Q}_i]_i = \begin{bmatrix} \cos\theta_i & -\lambda_i \sin\theta_i & \mu_i \sin\theta_i \\ \sin\theta_i & \lambda_i \cos\theta_i & -\mu_i \cos\theta_i \\ 0 & \mu_i & \lambda_i \end{bmatrix}$$

with

$$\lambda_i \equiv \cos\alpha_i, \quad \mu_i \equiv \sin\alpha_i$$

Furthermore, the orientation of the EE is given by:

$$\mathbf{Q} = \mathbf{Q}_1\mathbf{Q}_2\mathbf{Q}_3\mathbf{Q}_4\mathbf{Q}_5\mathbf{Q}_6 \tag{1}$$

while the position P of its operation point is given by:

$$\begin{aligned} \mathbf{p} &\equiv [\mathbf{p}]_1 \\ &= [\mathbf{a}_1]_1 + [\mathbf{a}_2]_1 + [\mathbf{a}_3]_1 + [\mathbf{a}_4]_1 + [\mathbf{a}_5]_1 + [\mathbf{a}_6]_1 \\ &= \mathbf{a}_1 + \mathbf{Q}_1(\mathbf{a}_2 + \mathbf{Q}_2\mathbf{a}_3 + \mathbf{Q}_2\mathbf{Q}_3\mathbf{a}_4 + \mathbf{Q}_2\mathbf{Q}_3\mathbf{Q}_4\mathbf{a}_5 + \mathbf{Q}_2\mathbf{Q}_3\mathbf{Q}_4\mathbf{Q}_5\mathbf{a}_6) \end{aligned} \tag{2}$$

The direct and inverse displacement analysis problems are both related to eqs. 1 and 2. Therefore, in the direct problem, the joints angles are known and the position and orientation of the EE are to be determined, while in the inverse problem it is the opposite.
The UR10e virtual laboratory suggests the following experiments, while not being limited to these experiments only:

- DDA where users will enter joints angles, see the robot moving accordingly, and validate their computation of EE position and orientation with those displayed in the control panel, under the DDA tab.
- IDA where users have to find the appropriate joints angles values allowing the robot to grasp a cube given at a known position and orientation, then enter these angles and check if the grasping is successful.
- PPO where users have to generate the appropriate $3-4-5$ polynomial trajectory to move the cube from point A to point B, then enter the coefficients of that computed polynomial, and check if the PPO application is successful.
- 3D Rotation understanding where users will go thoroughly in the computation of (i) Euler angles, (ii) Quaternions, and (iii) corresponding rotation matrix and validate their results while observing the orientation of the EE.

The control panel of the UR10e is divided into two sections: the yellow background section where the references values are entered, and the gray background section, where the robot's feedback is displayed in real-time. In the latter, the LED indicators are displayed and turn red when a joint exceeds its maximum range, alerting the user about a faulty maneuver. The panel is shown in Fig.7.

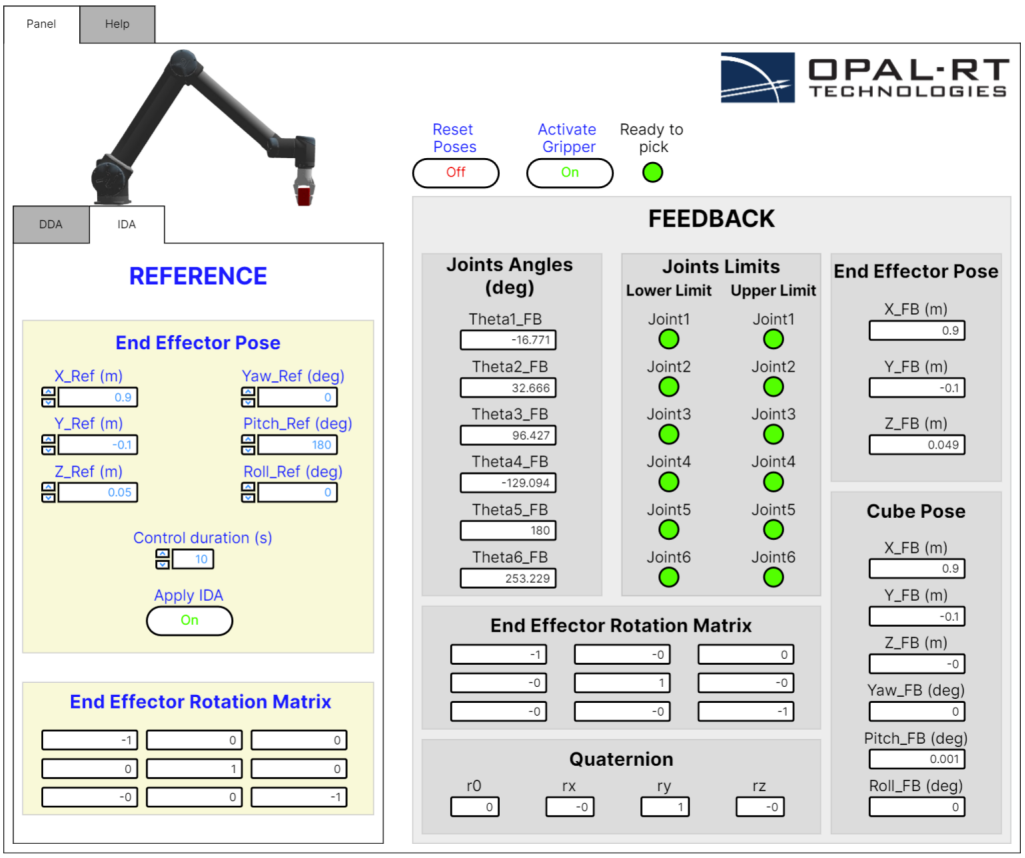

Figure 7: UR10e Control Panel with focus on IDA tab

In the sequel, the focus will be on the IDA experiment to grasp a red cube located on the table.For that:

1. Go to the ”IDA” tab.
2. Enter the position and orientation of the cube in the Reference section as follows: $x = 0.9$ m, $y = -0.1$ m, $z = 0.05$ m, yaw = 0 deg, pitch = 180 deg and roll = 0 deg.
3. Click on the ”Apply IDA” button.
4. Observe that the robot is moving from its initial pose towards the cube
5. Wait until the LED labeled ”Ready to pick” turn green, as this indicates that IDA is achieved and the robot attained the cube
6. Check that the joints angles values in the Feedback coincide with those calculated
7. Check that the EE pose in the Feedback coincide with the EE pose in the reference

8. Check that the EE rotation matrix in the Feedback corresponds to EE Rotation in the reference

9. Click on the ”Activate Gripper” button to grasp the cube.

5 Wheeled Mobile Pendulum Virtual Laboratory

A Mobile Wheeled Pendulum (MWP) is composed of three rigid bodies: two wheels that are driven separately and a central body. Depending on the position of the center of mass of the central body with respect to the line of wheels centers, the pendulum can be considered as inverted or non-inverted. In the case of the MWP virtual laboratory presented here, the battery is located on top inside the torus, rendering the pendulum an inverted one, as shown in Fig. 8. Additionally, this virtual robot is the digital twin of InPeRo [11]. Unlike other wheeled mobile robots, which contain three or more wheels, where the kinematics model is sufficient to achieve navigation maneuvers, the control design of MWP requires taking into account the dynamics model; otherwise, the system will suffer from unstable zero dynamics.

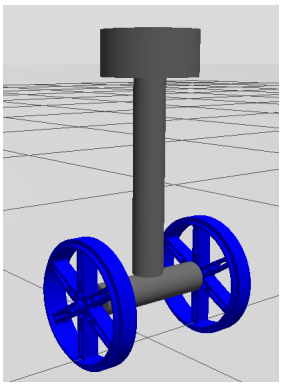

Figure 8: Inverted mobile wheeled pendulum

The MWP controller has been elaborated previously in [19] . It consists of three imbricated loops, as shown in Fig. 9.

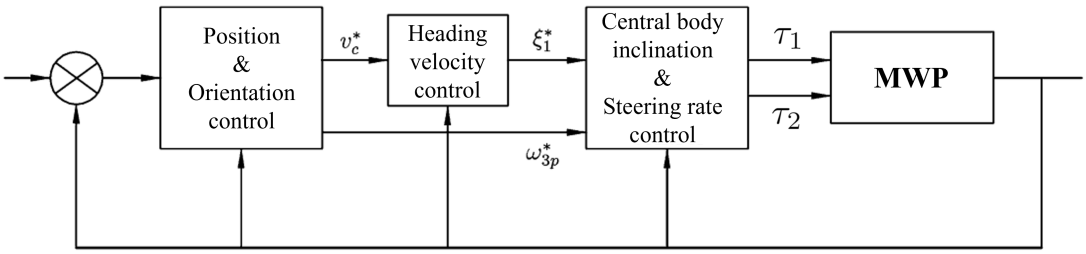

Figure 9: Representation of the control scheme

Inner Loop: This loop is responsible for controlling the inclination of the central body, ξ_1, and the robot steering rate ω_{3p} using the torques applied to the wheels.
Intermediate Loop: This loop shows the direct relationship between the robot heading acceleration and the central body inclination. For that, the aim of the control here is to use the heading speed to dictate the reference of the central body inclination [20].
External Loop: This loop is responsible for positioning and orienting the robot. The navigation algorithm used is based on a Lyapunov function for navigation and control in sliding mode as [21].

The MWP virtual laboratory suggest the following experiments:

- Use the inner loop to control the inclination of the central body, by applying ξ_1^*.
- Use the inner loop to control the steering rate, by applying ω_{3p}^*.
- Use the intermediate loop to control the inclination of the central body based on the heading speed v_c^* value.
- Use the External loop to control the position and orientation of the robot using the Lyapunov function for navigation and sliding mode control.

The control panel of the MWP is divided into three sections: the yellow background section where the reference values are entered, the gray background section, where the robot's feedback is displayed in real time, and the bottom section, where graphs are displayed for each of the three imbricated loops. The panel is shown in Fig.10.

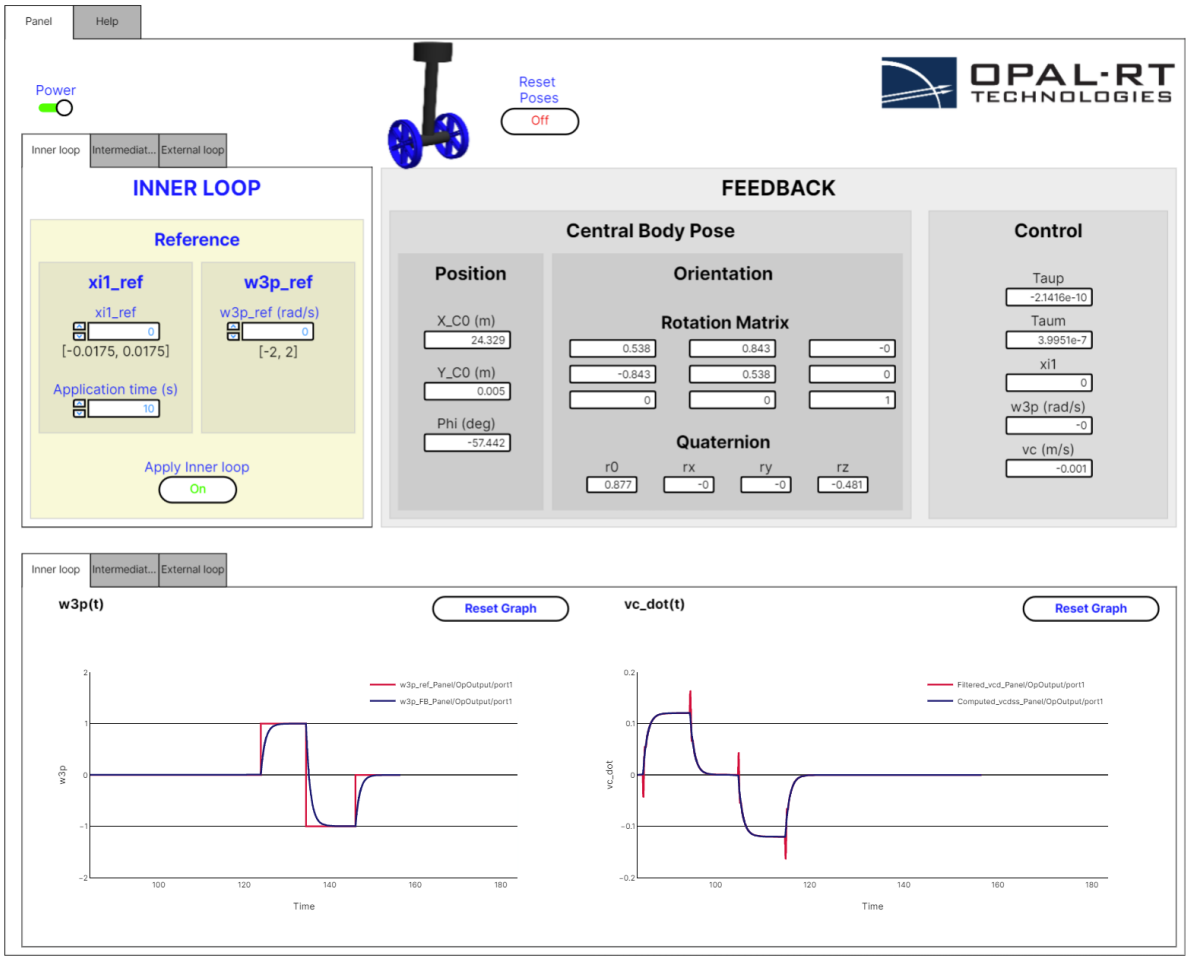

Figure 10: MWP Control Panel with focus on Inner loop tab

In the sequel the focus will be on the inner loop experiment to (i) control the inclination of the center body and (ii) to control the robot's steering angle. For that:

1. Go to the "xi1_ref" section under the "Inner loop" tab.
2. Set "xi1_ref" to -0.0175.
3. Set "Application time (s)" to 10.
4. Click the "Apply Inner loop" button to activate the control.
5. After 35 seconds, ξ_1^* will be applied for only 10 seconds, as specified in the application time above.
6. Visualize and interpret the graph of "vc_dot(t)" in the "Inner loop" graph tab, along with "xi1" in the feedback section.
7. Repeat the same steps, but this time set "xi1_ref" to 0.0175.

8. Observe that the robot comes to a complete stop, resulting in a zero heading speed at the end of these two tests.
9. Reset ”xi1_ref” back to 0 and set ”w3_p” to 1 rad/s to observe the robot moving in the counterclockwise direction.
10. Visualize and interpret the graph of ”w3_p(t)” under the ”Inner loop” graph tab.
11. Repeat the same steps for ”w3_p” and set it to -1 rad/s.

Furthermore, Fig.11 below shows the correspondence between the real and the virtual MWP when moving along a straight line with a trapezoidal heading speed profile. It is expected to have more noise on the real prototype as its virtual counterpart did not include yet the noise on sensors. Additionally, in terms of pitch angle, the virtual robot is behaving in a fully symmetrical way when accelerating and decelerating while its real counterpart is showing slight differences because despite all the attention given while constructing it, one cannot ensure full symmetry on both wheels and actuator mechanism.

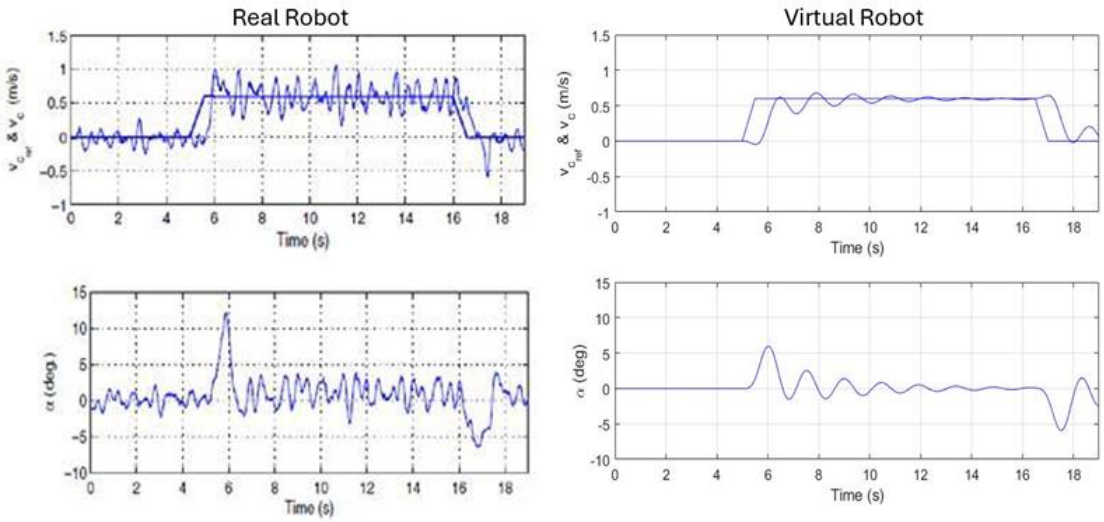

Figure 11: Comparison of results: real vs virtual MWP robots controlled to follow a straight line path

6 List of All Virtual Laboratories Developed in this Framework

As mentioned previously, this paper presented four virtual laboratories while 31 additional have been developed using the same framework. An exhaustive list is given below:

6.1 Electrical Virtual Laboratories

Fundamentals of Electrical Engineering

1. Single- and three-phase systems
2. Single- and three-phase transformer
3. Harmonics Analysis

Electric Machines

1. Synchronous Machine
2. Asynchronous Machine
3. Tansient Stability

Power Electronics

1. Boost Converter
2. Buck Converter
3. Buck Boost Converter
4. Single-phase Diode Rectifier
5. Single-phase Two-level Inverter
6. Three-phase Diode Rectifier
7. Three-phase Three-level Converter
8. Three-phase Thyristor Rectifier
9. Three-phase Two-level Inverter

Motor Drives

1. Brushed-DC Motor Drive
2. Squirrel-Cage Induction Motor Drive
3. Permanent Magnet Synchronous Motor Drive
4. Doubly Fed Induction Motor Drive

Renewable Energy

1. Battery Energy Storage System
2. Photovoltaic Generation System
3. Wind Turbine Generation System
4. Microgrid System

6.2 Robotics Virtual Laboratories

Serial Robotics Manipulators

1. 3-DOF Planar Robot
2. 6-DOF Spatial Decoupled Manipulator FANUC LRMate 200 iC
3. 6-DOF Spatial non Decoupled Manipulator UR10e.

Parallel Robotics Manipulators

1. 3-DOF Parallel Planar Robot
2. 6-DOF Stewart platform

Wheeled Mobile Robots

1. Differential Drive Robot
2. Ackermann-based Steering Robot
3. Articulated-based Robot
4. Mobile Wheeled Pendulum

Autonomous Off-road Vehicles

1. DDR combined to UR10e
2. Ackermann-based Steering Tractor Combined to a 3-DOF Serial Mower Arm
3. Articulated-based Steering Tractor Combined to a 2-DOF Serial Loader

7 Conclusions and Future Work

This paper presented four virtual laboratories, namely the synchronous machine, microgrid, serial robotic manipulator UR10e, and mobile wheeled pendulum, and enumerated the remaining 31 that were developed using the same spirit. Suggested laboratory exercises for all these virtual systems can be found here: https://opal-rt.atlassian.net/wiki/spaces/PCOURSEWARE/overview. The following features were adopted when designing these laboratories: interactivity, real thing, reset and repeatability, flexibility, self-learning, accessibility, scaling experiments, cost efficiency, safety, and bridging theory and practice. The feedback of the students was analyzed and other surveys/suggestions will follow to continue enhancing this experience. In the future, the development of virtual laboratories can be expanded to include other engineering disciplines, such as mechanical systems, allowing for a wider spectrum of educational opportunities. This could include simulations for studying complex mechanical dynamics, providing students with a well-rounded, interdisciplinary approach to engineering education. Such advancements would further enhance the versatility and impact of virtual laboratories in the preparation of future professionals.

References

[1] I. Veza, A. Sule, N. R. Putra, M. Idris, I. Ghazali, I. Irianto, U. Pendit, G. Mosliano, and A. Arasmatusy, *Virtual laboratory for engineering education: Review of virtual laboratory for students learning*, *Eng. Sci. Lett.*, vol. 1, no. 2, pp. 41-46, 2022.

[2] C. Nwosisi, A. Ferreira, W. Rosenberg, and K. Walsh, *A study of the flipped classroom and its effectiveness in flipping thirty percent of the course content*, Int. J. Inf. Educ. Technol., vol. 6, pp. 348-351, 2016

[3] J. García-Ferrero, R. P. Merchán, J. M. Mateos Roco, A. Medina, and M. J. Santos, *Towards a sustainable future through renewable energies at secondary school: An educational proposal*, *Sustainability*, vol. 13, no. 22, pp. 12904, 2021.

[4] S. Saovakhon and S. Akatimagool, *Development of innovative virtual media set for learning renewable energy*, in *2024 12th International Electrical Engineering Congress (iEECON)*, pp. 1-4, 2024.

[5] M. Daoudi, *Education in renewable energies: A key factor of Morocco's 2030 energy transition project. Exploring the impact on SDGs and future perspectives*, *Soc. Sci. & Hum. Open*, vol. 9, pp. 100833, 2024.

[6] R. O. Salcedo, J. K. Nowocin, C. L. Smith, R. P. Rekha, E. G. Corbett, E. R. Limpaecher, and J. M. LaPenta, *Development of a real-time hardware-in-the-loop power systems simulation platform to evaluate commercial microgrid controllers*, Lincoln Laboratory, MIT, Boston, MA, Tech. Rep. TR-1203, 2016.

[7] J. A. Restrepo-Zambrano, J. M. Ramírez-Scarpetta, M. L. Orozco-Gutiérrez, and J. A. Tenorio-Melo, *Experimental framework for laboratory scale microgrids*, *Rev. Fac. Ing. Univ. Antioquia*, vol. 81, pp. 9–23, 2016.

[8] R. Pastor, A. Llanos Tobarra, A. Robles-Gómez, J. Cano, B. Hammad, A. Al-Zoubi, R. Hernández, and M. Castro, *Renewable energy remote online laboratories in Jordan universities: Tools for training students in Jordan*, *Renewable Energy*, vol. 149, pp. 749–759, 2020.

[9] L. Guo, M. Vengalil, N. M. M. Abdul, and K. Wang, *Design and implementation of virtual laboratory for a microgrid with renewable energy sources*, *Comput. Appl. Eng. Educ.*, vol. 30, no. 2, pp. 349–361, 2022.

[10] L. Guo, N. M. M. Abdul, M. Vengalil, K. Wang, and A. Santuzzi, *Engaging renewable energy education using a web-based interactive microgrid virtual laboratory*, *IEEE Access*, vol. 10, pp. 60972–60984, 2022.

[11] D. S. Nasrallah, S. Brisebois, and M. Saad, "Realization of an inverted pendulum robot using nonlinear control for heading and steering velocities," in *Ad-*

vances in Systems Science, J. Swiatek, A. Grzech, P. Swiatek, and J. M. Tomczak, Eds., Springer, Switzerland, pp. 119–129, 2014.

[12] C. Peqqueña Suni, E. Ruppert, and F. Fajoni, *A guide for synchronous generator parameters determination using dynamic simulations based on IEEE standards*, in *Proc. XIX Int. Conf. Electr. Mach. (ICEM)*, Rome, Italy, 2010, pp. 1–6, doi: 10.1109/ICELMACH.2010.5607986.

[13] M. Kamwa, H. Pilote, P. Carle, B. Viarouge, B. Mpanda-Mabwe, and M. Crappe, *Computer software to automate the graphical analysis of sudden-short-circuit oscillograms of large synchronous machines*, *IEEE Trans. Energy Convers.*, vol. 10, no. 3, pp. 399–406, Sep. 1995, doi: 10.1109/60.464860.

[14] A. Tabares, N. Martinez, L. Ginez, J. F. Resende, N. Brito, and J. F. Franco, *Optimal capacity sizing for the integration of a battery and photovoltaic microgrid to supply auxiliary services in substations under a contingency*, *Energies*, vol. 13, no. 22, p. 6037, 2020, doi: 10.3390/en13226037.

[15] M. Kesraoui, N. Korichi, and A. Belkadi, *Maximum power point tracker of wind energy conversion system*, Renewable Energy, vol. 36, no. 10, pp. 2655–2662, 2011.

[16] A. R. Reisi, M. H. Moradi, and S. Jamasb, *Classification and comparison of maximum power point tracking techniques for photovoltaic system: A review*, Renewable Sustainable Energy Rev., vol. 19, pp. 433–443, 2013.

[17] M. A. Abdulgalil, M. Khalid, and F. Alismail, *Optimal sizing of battery energy storage for a grid-connected microgrid subjected to wind uncertainties*, Energies, vol. 12, no. 12, p. 2412, 2019.

[18] J. Angeles, *Fundamentals of Robotic Mechanical System: Theory, Methods, and Algorithms*, 4th Edition, Springer, 2014

[19] D. S. Nasrallah, H. Michalska, and J. Angeles, "Controllability and posture control of a wheeled pendulum moving on an inclined plane," *IEEE Trans. Robotics*, vol. 23, no. 3, pp. 564–577, 2007.

[20] D. Nasrallah, J. Angeles, and H. Michalska, *Velocity and orientation control of an anti-tilting mobile robot moving on an inclined plane*, Proc. IEEE Int. Conf. Robot. Autom., 2006, pp. 3717–3723. doi: 10.1109/ROBOT.2006.1642270.

[21] J. Guldner and V. I. Utkin, "Stabilization of nonholonomic mobile robots using Lyapunov functions for navigation and sliding mode control," in Proc. 33rd Conf. Decision Control, Lake BuenaVista, FL, Dec. 1994, pp. 2967–2972